ISSN 0036-0244, Russian Journal of Physical Chemistry A, 2010, Vol. 84, No. 9, pp. 1485–1490. © Pleiades Publishing, Ltd., 2010.
Original Russian Text © I.K. Razumov, 2010, published in Zhurnal Fizicheskoi Khimii, 2010, Vol. 84, No. 9, pp. 1632–1637.

CHEMICAL THERMODYNAMICS AND THERMOCHEMISTRY

The Synthesis of Metastable Phases in Plastic Deformation of Alloys

I. K. Razumov

Institute of Metal Physics, Ural Division, Russian Academy of Sciences, Yekaterinburg
e-mail: iraz@k66.ru

Received September 23, 2009

Abstract—Intense plastic deformation caused by intragrain edge dislocation slip can contribute to the decomposition of equilibrium and formation of metastable phases in the volume of grains. The effect is caused by local changes in the thermodynamic properties of alloys and acceleration of diffusion in the region of a dislocation core. As a consequence, mechanical dislocation slip energy transforms into internal alloy energy, and the nonequilibrium state of the resulting alloy is "frozen."

DOI: 10.1134/S0036024410090062

INTRODUCTION

Anomalous phase transformations that occur in alloys because of intense plastic deformation attract increased interest of researchers [1–8], who hope to obtain promising materials by this method [9]. Experiments show that, under intense plastic deformation conditions, an alloy moves from the state of thermodynamic equilibrium, and part of mechanical energy supplied to the system transforms into internal alloy energy [10, 11]. The mechanisms responsible for this process are, however, debatable [1, 12, 13]. Among several factors that influence the phase stability of alloys during intense plastic deformation (direct mechanical mixing of atoms in deformation bands, the action of nonequilibrium vacancy fluxes, the disturbance of crystalline order close to grain boundaries, etc.), intragrain edge dislocation slip, which occurs no matter how an alloy is deformed, should be mentioned.

Indeed, according to modern concepts, plastic deformation transfer between neighboring crystallites does not stop even during alloy transition to the amorphous state and the formation of nonequilibrium grain boundaries [14]. Local changes in thermodynamic properties cause the formation of Cottrell atmospheres in dislocation tubes [15], the appearance of extended impurity traces behind moving dislocations [16], and the local solution of precipitates intersected by dislocations [17–19]. The rate of diffusion in a dislocation core is higher by 2–3 orders of magnitude than that in the volume [20], and it can be suggested that the nonequilibrium alloy state gets frozen after dislocation shift until the next dislocation arrives, which provokes the further development of nonequilibrium transformations. The formation of metastable phase diagram phases in this process is preferable compared with the formation of fundamentally new phases, because metastable states correspond to local minima of the free energy of mixing and are therefore long-lived. In this work, the qualitative peculiarities of the synthesis of metastable phases under intense plastic deformation conditions are studied for the example of an alloy with a tendency to B2 ordering.

MODEL

Diffusion equations for an alloy with a tendency to B2 ordering were suggested in [21] and used in [22] to study the growth of colonies; the results were consistent with Monte Carlo simulations. The evolution of the concentration of component A is described by the continuity equation

$$dc_A/dt = -\nabla \mathbf{J}_A. \quad (1)$$

The flux of component A is determined as

$$\mathbf{J}_A = -D\left[\left(1-\Psi c_A^{(1)}c_B^{(1)}\right)\nabla c_A + \left(1-\Xi c_A^{(1)}c_B^{(1)}\right)\nabla \eta_A\right] + Dc_A^{(1)}c_B^{(1)}\left[\frac{R^2}{2}\nabla\left(\Xi\Delta\eta_A + \Psi\Delta c_A\right)\right] + \Lambda, \quad (2)$$

$$\Lambda = Dc_A^{(1)}c_B^{(1)}\left[-\frac{\nabla\phi}{2} + \left(c_A - \frac{1}{2}\right)\nabla\Psi + \eta_A\nabla\Xi\right],$$

where D is the diffusion coefficient; $c_\sigma^{(1,2)}$ stands for the sublattice concentrations of atoms of kinds $\sigma = A, B$; and Ψ and Ξ are the energies of mixing and ordering divided by the thermal energy kT. For simplicity, energy ϕ will be set equal to zero. The mean local concentration and the degree of ordering are determined by the equations $c_\sigma = \left(c_\sigma^{(1)} + c_\sigma^{(2)}\right)/2$ and $\eta_\sigma = \left(c_\sigma^{(1)} - c_\sigma^{(2)}\right)/2$. We assume that the contribution to flux Λ is only nonzero in the region of dislocation cores because of a local change in thermodynamic

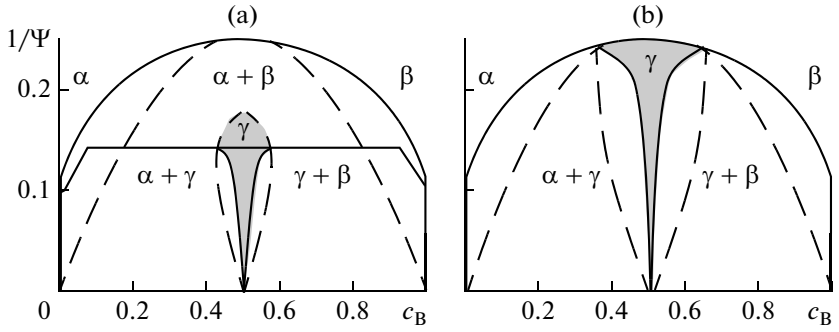

Fig. 1. Phase diagrams of alloys with (a) metastable and (b) equilibrium ordered γ phase. Phase equilibrium curves and spinodals are given by solid and dashed lines, respectively; Ψ/Ξ = (a) 1.2 and (b) 0.8.

properties. The η_σ value is determined in the local-equilibrium ordering approximation by the Bragg–Williams condition

$$c_A^{(2)}c_B^{(1)} = c_A^{(1)}c_B^{(2)}\exp\left[-2\Xi\left(\eta_A + R^2\Delta\eta_A/2\right)\right].$$

If Ξ = 0 and Λ = 0, Eq. (2) reduces to the Cahn–Hilard equation [23], which can be used to describe the spinodal decomposition of a regular solid solution,

$$J_A = -D(1-\Psi c_A c_B)\nabla c_A + DR^2\Psi c_A c_B(\nabla\Delta c_A)/2.$$

If a local-equilibrium ordering is not reached on the time scale under consideration, the evolution of the order parameter should be considered [21],

$$\frac{d\eta_A}{dt} = \frac{DQ}{a^2}\left[c_A^{(2)}c_B^{(1)} - \frac{\omega_A^{(1)}\omega_B^{(2)}}{\omega_A^{(2)}\omega_B^{(1)}}c_A^{(1)}c_B^{(2)}\right], \qquad (3)$$

where Q is the correction factor, a is the lattice parameter, and $\omega_\sigma^{(1,2)}$ stands for the diffusion mobilities of atoms in sublattices.

Typical phase diagrams of the model under consideration are shown in Fig. 1. The dark region corresponds to a metastable phase if Ψ > Ξ (Fig. 1a) and a stable ordered phase if Ψ < Ξ (Fig. 1b). In the first case, alloy cooling below the dome of the two-phase region causes alloy decomposition into equilibrium phases α and β enriched in atoms of kinds A and B, respectively. The decomposition of the metastable γ phase requires activation and develops by the mechanism of the growth of colonies or double plates from regions with disturbed homogeneity [22]. In the second case, the phase diagram has two two-phase regions α + γ and β + γ each experiencing spinodal decomposition with the precipitation of the ordered γ phase.

The term Λ ≠ 0 in (2) contributes to alloy removal from thermodynamic equilibrium, and, for intense plastic deformation, preferable transformation can be α + β → γ for the first case and ordered phase decomposition γ → α + β for the second case. The observation of one or another scenario depends on energy gradients $\nabla\Psi, \nabla\Xi, \nabla\phi$ in a dislocation core, that is, on the properties of the material. For crude qualitative analysis purposes, we assume that a change in the Gibbs energy is independent of the sign of deformation and ignore differences in Ψ, Ξ energy and diffusion coefficient changes in the regions of dislocation core compression and expansion. These parameters are determined phenomenologically in a dislocation core using the radially symmetrical functions

$$D = D_0(1+\delta_D\xi), \quad \Psi = \Psi_0(1+\delta_\Psi\xi),$$
$$\Xi = \Xi_0(1+\delta_\Xi\xi), \quad \xi = \left[1+\left(\left(\mathbf{r}-\mathbf{r}_0(t)\right)/\left(L\delta_L\right)\right)^4\right]^{-1}, \qquad (4)$$

where δ_D, δ_Ψ, and δ_Ξ characterize the amplitude and $\xi(\mathbf{r})$ the form of parameter perturbation in a dislocation core; the position of a dislocation is determined by the $\mathbf{r}_0(t)$ radius vector.

SIMULATION RESULTS

Equations (1)–(4) were numerically solved by the standard Runge–Kutta method on an $L \times L$ square region. It was assumed that grain boundaries coincided with the boundaries of the square and atom fluxes through them were absent. The initial state was selected homogeneous or two-phase equilibrium with small composition fluctuations. A dislocation appeared randomly at one of the boundaries, moved to the opposite boundary at a constant rate V, and disappeared at this boundary. At the same moment, new dislocation was generated, and a single dislocation was present in the sample at any time moment. Various levels of the concentration of component A are shown in Figs. 2–4 by various shades of gray, and ordered phase precipitates are hatched. The integral degrees of alloy decomposition, dispersity, and ordering are determined by the $\langle S\rangle$, $\langle F\rangle$, and $\langle\eta\rangle$ values, respectively,

$$\langle S\rangle = \int\left|c_A(\mathbf{r}) - \langle c_A\rangle\right|d\mathbf{r}\Big/2\langle c_A\rangle\langle c_B\rangle L^2,$$
$$\langle F\rangle = \int\left|\nabla c_A(\mathbf{r})\right|d\mathbf{r}\Big/L^2, \qquad (5)$$
$$\langle\eta\rangle = \int\left|\eta_A(\mathbf{r})\right|d\mathbf{r}\Big/L^2\langle c_A\rangle, \quad \langle c_\sigma\rangle = \int\frac{c_\sigma(\mathbf{r})}{L^2}d\mathbf{r}.$$

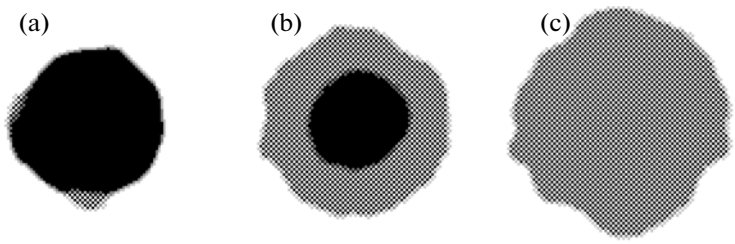

Fig. 2. Solution of equilibrium phases and synthesis of a metastable ordered phase caused by the passage of (a) 150, (b) 4000, and (c) 8000 dislocations through a grain; $VL/D_0\delta_D = 100$, $\Psi = 7.2$, $\Xi = 6$, $\delta_\Psi = -0.5$, $\delta_\Xi = 0$, $\delta_D = 10^2$, $\delta_L = 0.05$, $R/L = 0.015$, and $a^2/QL^2 \approx 0$.

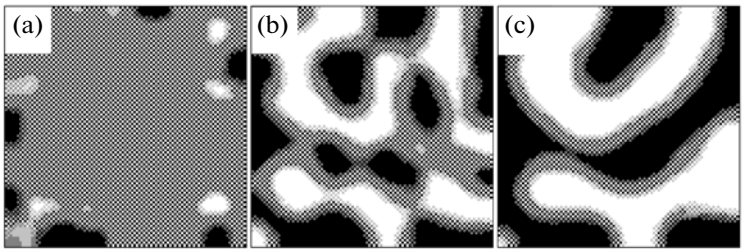

Fig. 3. Decomposition of an equilibrium ordered phase caused by the passage of (a) 200, (b) 1000, and (c) 2000 dislocations through a grain; $VL/D_0\delta_D = 50$, $\Psi = 5$, $\Xi = 6$, $\delta_\Psi = 0$, $\delta_\Xi = -1$, $\delta_D = 10^3$, $\delta_L = 0.05$, $R/L = 0.015$, and $a^2/QL^2 \approx 0$.

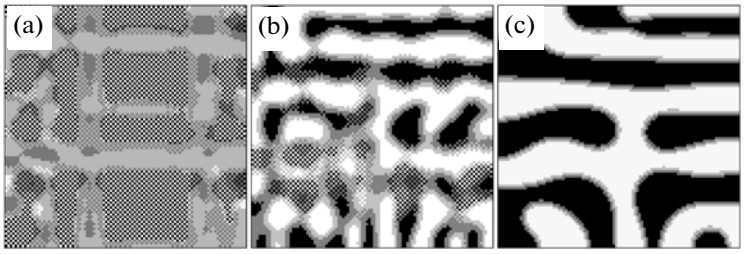

Fig. 4. Decomposition of an equilibrium ordered phase caused by the passage of (a) 25, (b) 100, and (c) 1000 dislocations through a grain; $VL/D_0\delta_D = 50$, $\Psi = 5$, $\Xi = 6$, $\delta_\Psi = 0$, $\delta_\Xi = -1$, $\delta_D = 10^3$, $\delta_L = 0.05$, $R/L = 0.015$, and $a^2/QL^2 = 10^{-4}$.

The kinetics of solution of an equilibrium phase precipitate in an alloy with the phase diagram corresponding to Fig. 1a as the energy of mixing Ψ in a dislocation core decreases is shown in Fig. 2. At the initial stage, the matrix is enriched in atoms of kind A because of their entrainment with dislocations that intersect the precipitate. After an incubation period, a nucleus of the γ phase appears at the boundary between the α - and β phases (Fig. 2a). Phase γ rapidly envelops the initial precipitate (Fig. 2b), and the volume fraction of the γ phase then increases to saturation (Fig. 2c). It should be expected that the rate of the return to equilibrium during annealing after action must depend on the degree of $\alpha + \beta \rightarrow \gamma$ nonequilibrium transformation, because the decomposition of the metastable γ phase is only possible from regions with disturbed homogeneity [22].

The kinetics of the decomposition of the equilibrium ordered γ phase (phase diagram corresponds to Fig. 1b) as the energy of ordering Ξ decreases in the dislocation core is shown in Fig. 3. At the initial stage, α and β phase precipitates appear close to the boundaries of the square under consideration (Fig. 3a). The transformation then extends deep in the grain (Fig. 3b), and, if the action is long, a state is reached in which nonequilibrium α and β phase precipitates are separated by γ phase interlayers (Fig. 3c). It follows that competition between the external action and stimuli to return to equilibrium results in the formation of a band dissipative structure. If in addition the relaxation time of order parameter η after dislocation

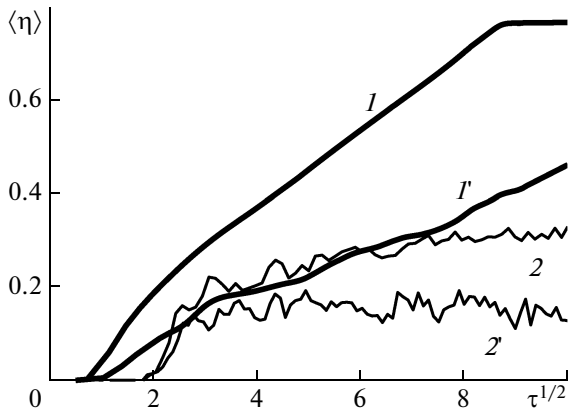

Fig. 5. Evolution of the degree of ordering with time; $VL/D_0\delta_D$ = (*1*, *1*') 100 and (*2*, *2*') 30, δ_D = (*1*, *2*) 100 and (*1*', *2*') 75, $\Psi = 7.2$, $\Xi = 6$, $\delta_\Psi = -0.5$, $\delta_\Xi = 0$, $\delta_L = 0.05$, $R/L = 0.015$, and $a^2/QL^2 \approx 0$.

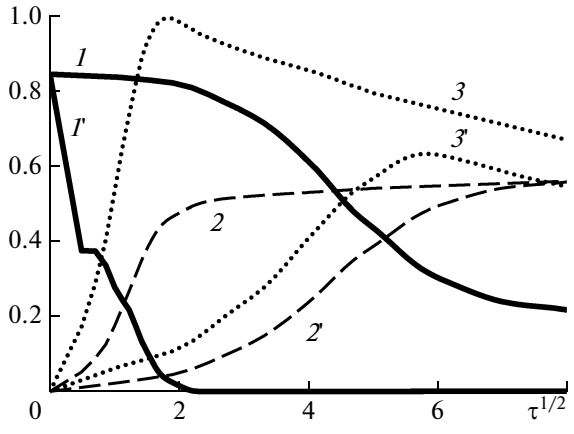

Fig. 6. Evolution of (*1*, *1*') the degree of ordering ⟨η⟩, (*2*, *2*') decomposition ⟨*S*⟩, and (*3*, *3*') dispersity ⟨*F*⟩ of an alloy with time at (*1*–*3*) fast and (*1*'–*3*') slow order parameter η relaxation; $VL/D_0\delta_D = 50$, $\Psi = 5$, $\Xi = 6$, $\delta_\Psi = 0$, $\delta_\Xi = -1$, $\delta_D = 10^3$, $\delta_L = 0.05$, $R/L = 0.015$, and a^2/QL^2 (*1*–*3*) ≈ 0 and (*1*'–*3*') 10^{-4}; the ⟨*F*⟩ (*t*) curves are normalized by the maximum ⟨*F*⟩ value.

passage is comparable with the characteristic time of the approach of a new dislocation to this region, alloy decomposition is preceded by partial disordering, and, after prolonged action, γ phase interlayers are absent (see Fig. 4). Such a situation can only arise at low temperatures, when diffusion in the volume is fully frozen. In both cases, the state formed can conventionally be called metastable, because the α and β phases correspond to local Gibbs energy minima and are present in the equilibrium phase diagram (Fig. 1b). However, the return to the equilibrium state during annealing does not require activation.

The evolution of integral transformation characteristics (see Eqs. (5)) is shown in Figs. 5 and 6. Time is given in dimensionless units $\tau = D_0\delta_D N_d/LV$, where N_d is the number of dislocations passed through the grain. Figure 5 shows that the kinetics of growth of metastable γ phase precipitates is similar to the Avrami kinetics [24] and includes such characteristic stages as incubation period, exhaustion of nucleation sites (accompanied by a change in the curve slope), the linear growth of a new phase layer, and saturation. Interestingly, growth rate is almost independent of the size of the residual α phase precipitate to its complete solution (curve *1*). A decrease in the δ_D and *V* parameters decelerates the transformation and increases fluctuations (compare curves *1*, *2* and *1*', *2*'), and stationary conditions are reached at incomplete precipitate solution (curve *2*').

Additional calculations show that there are critical δ_D and *V* values at which equilibrium phases remain stable. Figure 6 shows that the decomposition of the equilibrium γ phase under the action of dislocations is substantially accelerated and a more dispersed state can be reached if the relaxation time of the order parameter η is long (compare curves *1* and *1*'). Disordering then proceeds in two stages, which is seen as a change in the slope of the ⟨η⟩(*t*) curve. The fast disordering stage develops in times determined by the rate of dislocation movement, and the slow stage is possible because of alloy decomposition; it is controlled by diffusion through distances on the order of the size of precipitates. The evolution of the degree of decomposition and dispersity (see curves *2*, *2*' and *3*, *3*') is qualitatively similar to the kinetics of spinodal decomposition [25] and includes the growth of fluctuations, fast wave stage, coalescence of precipitates (close to the ⟨*F*⟩(*t*) curve maximum), and slow growth of large precipitates because of the vaporization of smaller ones. Additional calculations show that the δ_D value should be higher than its critical value; otherwise, the equilibrium phase remains stable.

RESULTS AND DISCUSSION

It was shown that, under the conditions of intense plastic deformation, an alloy moved away from the state of thermodynamic equilibrium because of local changes in thermodynamic properties and diffusion acceleration in the region of moving dislocation cores. The synthesis of metastable phases and nonequilibrium disperse structures was then possible. The character of transformations depended on the material and was determined by interatomic interaction energy gradients in the dislocation core. Experimental estimates for cementite Fe_3C [26], iron nitride Fe_4N [27], and some substitution alloys such as Ni_3Al [18, 19] showed that the binding energy between an impurity and dislocation could exceed the phase formation energy. Theoretical estimates were performed ab initio; it was,

for instance, shown [28] that the interaction energy between the As atom and dislocation in Si was of ~1 eV, and As atoms were ordered in the dislocation tube.

Nonequilibrium transformations of the dislocation nature were likely observed experimentally [1–4]. In [1], the solution of Ni_3Me (Ti, Al, Si, and Zr) intermetallic compounds in Fe–Ni–Me face-centered cubic matrices was studied. It was shown that the fraction of dissolved nickel atoms linearly depended on the degree of true deformation proportional to the dislocation flux. In [2], intense plastic deformation of pearlitic steel U13 by shear under pressure at room temperature caused the solution of cementite Fe_3C with the formation of metastable ε and χ carbides according to the scheme $\alpha\text{-Fe} + Fe_3C \longrightarrow \alpha\text{-Fe–C} \longleftrightarrow \varepsilon + \chi + \gamma\text{-Fe–C}$. In [3], the mechanically induced solution of equilibrium nitride Fe_4N with the formation of the $Fe_{16}N_2$ metastable compound was observed,

$$\alpha\text{-Fe} + Fe_4N \longrightarrow \alpha\text{-Fe–N} + \gamma\text{-Fe–N} + Fe_{16}N_2 + Fe_4N.$$

In [4], intense plastic deformation-induced dynamic solution of oxides proceeded as

$$\alpha\text{-}Fe_2O_3 + Me \longrightarrow Fe_{3-y}O_4 + Fe_{1-x}O + Fe\text{–}O + Me\text{–}Fe + Me\text{–}Fe\text{–}O + \alpha\text{-Fe–Me},$$

where Me is the matrix of metals; after post-deformation annealing, the $Fe_{3-y}O_4$ and $Fe_{1-x}O$ metastable oxides disappeared.

There are also many experimental observations that remain unexplained or are interpreted not unambiguously [5–8]. For instance, in [5], the decomposition of equilibrium solid solutions was observed when $La_{50}Ag_{50}$, $La_{38}Co_{62}$, $La_{34}Ni_{66}$, $Cr_{50}Zr_{50}$, etc. alloy powders were ground in a ball mill. The decomposition of the $Nd_2Fe_{14}B$ compound into nonequilibrium phases enriched in and depleted of Nd was observed on a Bridgman anvil [6]. The depth of decomposition increased as the degree of deformation grew, and it was shown that the initial state was recovered under annealing. In [7], similar decomposition of the Fe_2B equilibrium compound was observed. It was noticed that the intermetallic compound first experienced disordering and partially became amorphous, and only then did its stratification occur. Such a behavior is in qualitative agreement with the case considered above, when order parameter η relaxation cannot occur in time between dislocation passages (Fig. 4).

The formation of solid solutions under intense plastic deformation conditions in immiscible systems such as Cu–Co or Fe–Cu [8] cannot be explained by the action of fluxes of nonequilibrium vacancies [12] or grain boundary segregation [13], which can only change the morphology of precipitates. In view of this, Skakov suggested [10] that "exorbitatnt" solid solutions behaved as metastable phases at low temperatures; that is, their appearance was predetermined thermodynamically. By way of example, the data from [29] are given. In [29], the metastable character of the obtained supersaturated Cu–Ag solid solution was substantiated experimentally. In reality, this means that phase diagrams of many alloys at low temperatures remain poorly studied, and intense plastic deformation can be one of the main tools of synthesizing metastable phases in alloys.

ACKNOWLEDGMENTS

The author thanks A.E. Ermakov and Yu.N. Gornostyrev for useful discussions.

REFERENCES

1. V. V. Sagaradze, V. A. Shabashov, T. M. Lapina, et al., Fiz. Met. Metalloved. **78** (6), 49 (1994).
2. V. A. Shabashov, L. G. Korshunov, A. G. Mukoseev, et al., Mater. Sci. Eng. **346**, 196 (2003).
3. V. A. Shabashov, S. V. Borisov, A. E. Zamatovskii, et al., Fiz. Met. Metalloved. **102**, 582 (2006).
4. V. A. Shabashov, A. V. Litvinov, A. G. Mukoseev, et al., Fiz. Met. Metalloved. **98** (6), 38 (2004).
5. H. Bakker, P. I. Loeff, and A. W. Weeber, Def. Diff. Forum **66**, 1169 (1989).
6. V. S. Gaviko, A. G. Popov, A. S. Ermolenko, et al., Fiz. Met. Metalloved. **92** (2), 58 (2001).
7. C. E. Rodriquez Torres, F. N. Sanches, and L. A. Mendoza Zeilis, Phys. Rev. B **51**, 12142 (1995).
8. X. Sauvage, F. Wetscher, and P. Pareige, Acta Mater. **53**, 2127 (2005).
9. R. Z. Valiev and I. V. Aleksandrov, *Nanostructural Materials Produced by Severe Plastic Deformation* (Logos, Moscow, 2000) [in Russian].
10. Yu. A. Skakov, Metalloved. Term. Obrab. Met., No. 7, 45 (2005).
11. Yu. S. Nechaev, Diffusion Fundam. **2**, 52 (2005).
12. A. E. Ermakov, V. D. Gapontsev, V. V. Kondrat'ev, et al., Fiz. Met. Metalloved. **88** (3), 5 (1999).
13. I. K. Razumov and Yu. N. Gornostyrev, et al., J. Alloys Comp. **434**, 535 (2007).
14. S. V. Bobylev, M. Yu. Gutkin, and I. A. Ovid'ko, Fiz. Tverd. Tela **50**, 1813 (2008) [Phys. Solid State **50**, 1888 (2008)].
15. A. H. Cottrell, *Dislocations and Plastic Flow in Crystals* (Clarendon, Oxford, 1953; Metallurgizdat, Moscow, 1958).
16. V. G. Eremenko, V. I. Nikitenko, and E. B. Yakimov, Pis'ma Zh. Éksp. Teor. Fiz. **26** (2), 72 (1977).
17. B. Ya. Lyubov and V. A. Shmakov, Fiz. Met. Metalloved. **29**, 968 (1970).
18. H. Gleiter and E. Hornbogen, Phys. Stat. Solidi A **12**, 235 (1965).

19. H. Gleiter, Acta Metall. **16**, 455 (1968).

20. M. Legros, G. Dehm, E. Arzt, et al., Science **319** (5870), 1646 (2008).

21. I. K. Razumov, Inzh.–Fiz. Zh. **81**, 789 (2008).

22. I. K. Razumov, Zh. Fiz. Khim. **83**, 1865 (2009) [Russ. J. Phys. Chem. A **83**, 1682 (2009)].

23. J. W. Cahn, Acta. Metall **9**, 795 (1961).

24. J. Christian, *The Theory of Transformations in Metals and Alloys* (Pergamon, Oxford, 1965; Mir, Moscow, 1978).

25. V. G. Vaks, S. V. Veiden, and V. Yu. Dobretsov, Pis'ma Zh. Éksp. Teor. Fiz. **61**, 65 (1995) [JETP Lett. **61**, 68 (1995)].

26. I. I. Milinskaya and I. A. Tomilin, Fiz. Met. Metalloved. **26**, 21 (1968).

27. L. J. Dijkstra, J. Met. **185**, 252 (1949).

28. A. Maiti, Kaplan, M. Mostoller, et al., Appl. Phys. Lett. **70**, 336 (1997).

29. E. Ma, H. W. Sheng, J. H. He, et al., Mat. Sci. Eng. **286**, 48 (2000).